REPORT DOCUMENTATION PAGE

1

Form Approved OMB NO. 0704-0188

1. REPORT DATE (DD-MM-YYYY)	2. REPORT TYPE	3. DATES COVERED (From - To)
	New Reprint	-

4. TITLE AND SUBTITLE

Toward Strong Thermoplastic Elastomers with Asymmetric Miktoarm Block Copolymer Architectures

5a. CONTRACT NUMBER

5b. GRANT NUMBER

W911NF-09-D-0001

5c. PROGRAM ELEMENT NUMBER

611104

6. AUTHORS

Weichao Shi, Nathaniel A. Lynd, Damien Montarnal, Yingdong Luo, Glenn H. Fredrickson, Edward J. Kramer, Christos Ntaras, Apostolos Avgeropoulos, Alexander Hexemer

5d. PROJECT NUMBER

5e. TASK NUMBER

5f. WORK UNIT NUMBER

7. PERFORMING ORGANIZATION NAMES AND ADDRESSES

University of California - Santa Barbara
3227 Cheadle Hall
3rd floor, MC 2050
Santa Barbara, CA 93106 -2050

8. PERFORMING ORGANIZATION REPORT NUMBER

9. SPONSORING/MONITORING AGENCY NAME(S) AND ADDRESS (ES)

U.S. Army Research Office
P.O. Box 12211
Research Triangle Park, NC 27709-2211

10. SPONSOR/MONITOR'S ACRONYM(S)

ARO

11. SPONSOR/MONITOR'S REPORT NUMBER(S)

55012-LS-ICB.716

12. DISTRIBUTION AVAILIBILITY STATEMENT

Approved for public release; distribution is unlimited.

13. SUPPLEMENTARY NOTES

The views, opinions and/or findings contained in this report are those of the author(s) and should not contrued as an official Department of the Army position, policy or decision, unless so designated by other documentation.

14. ABSTRACT

See Attached

15. SUBJECT TERMS

See Attached

16. SECURITY CLASSIFICATION OF:			17. LIMITATION OF ABSTRACT	15. NUMBER OF PAGES	19a. NAME OF RESPONSIBLE PERSON
a. REPORT	b. ABSTRACT	c. THIS PAGE			Francis Doyle
UU	UU	UU	UU		19b. TELEPHONE NUMBER 805-893-8133

Report Title

Toward Strong Thermoplastic Elastomers with Asymmetric Miktoarm Block Copolymer Architectures

ABSTRACT

See Attached

REPORT DOCUMENTATION PAGE (SF298)
(Continuation Sheet)

Continuation for Block 13

ARO Report Number 55012.716-LS-ICB
Toward Strong Thermoplastic Elastomers with A...

Block 13: Supplementary Note

Approved for public release; distribution is unlimited.

Macromolecules

Article

pubs.acs.org/Macromolecules

Toward Strong Thermoplastic Elastomers with Asymmetric Miktoarm Block Copolymer Architectures

Weichao Shi,[†] Nathaniel A. Lynd,[†] Damien Montarnal,[†] Yingdong Luo,[†] Glenn H. Fredrickson,*[,†,‡] and Edward J. Kramer*[,†,‡,§]

[†]Materials Research Laboratory, [‡]Department of Chemical Engineering, and [§]Department of Materials, University of California at Santa Barbara, Santa Barbara, California 93106, United States

Christos Ntaras and Apostolos Avgeropoulos*

Department of Materials Science and Engineering, University of Ioannina, University Campus, Ioannina, Greece 45110

Alexander Hexemer

Advanced Light Source, Lawrence Berkeley National Laboratory, 1 Cyclotron Road, Berkeley, California 94720, United States

Supporting Information

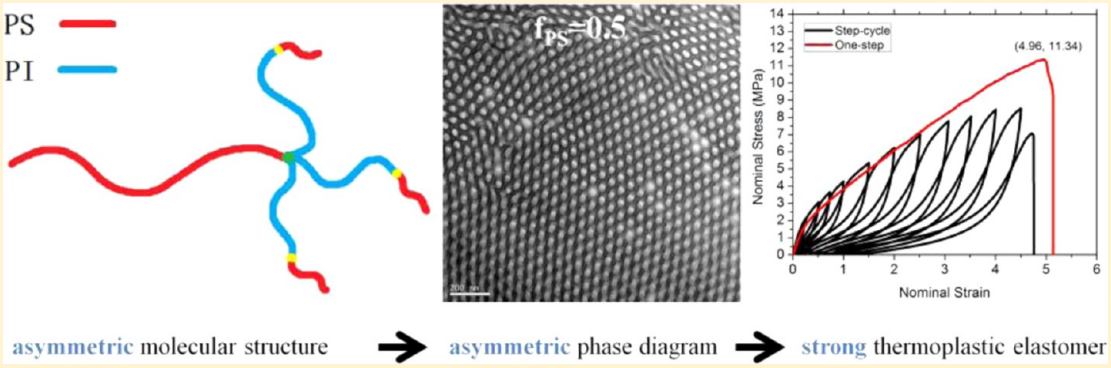

ABSTRACT: Thermoplastic elastomers (TPEs) are designed by embedding discrete glassy or semicrystalline domains in an elastomeric matrix. Typical styrenic-based amorphous TPEs are made of linear ABA-type triblock copolymers, where the volume fraction f of the glassy domains A is typically less than 0.3. This limitation ultimately restricts the range of mechanical strength attainable with these materials. We had previously predicted using self-consistent field theory (SCFT) that $A(BA')_n$ miktoarm block copolymers with an approximately 8:1 ratio of the A to A′ block molecular weights and $n \geq 3$ should exhibit discrete A domains at considerably larger f and offer potential for the combination of high modulus, high recoverable elasticity, and high strength and toughness. Using transmission electron microscopy and small-angle X-ray scattering on model polystyrene-*b*-polyisoprene (PS−PI) miktoarm copolymers, we show that such polymers indeed possess discrete PS domains for f values considerably higher than 0.3. The hexagonal morphology with PS cylinders was achieved for $f = 0.5$ and $n = 3$. Mechanical testing indicates that these miktoarm materials are strong, tough, and elastic and thus may be potential candidates for a new generation of thermoplastic elastomers.

INTRODUCTION

Thermoplastic elastomers are fascinating materials and have drawn much attention in industry. The polystyrene (PS)-based block copolymers are a dominant category in the family of commercial thermoplastic elastomers (TPEs). Typical examples are polystyrene−poly(butadiene)−polystyrene (SBS), polystyrene−poly(ethylene-*co*-butylene)−polystyrene (SEBS), and polystyrene−poly(isoprene)−polystyrene (SIS) linear triblock copolymers. The physical principles underlying the behavior of such copolymers are well understood.[1,2] The immiscibility between the PS (glass transition temperature $T_g \sim 110$ °C) and the polydiene or polyolefin (T_g below −50 °C) blocks leads to microphase separation on a 10 nm scale. The major elastomeric middle block is anchored by the minor glassy end blocks. The PS phase must stay discrete as it plays the role of physical cross-links in the elastomeric matrix, usually with spherical or

Received: December 16, 2013
Revised: February 10, 2014
Published: March 5, 2014

   dx.doi.org/10.1021/ma402566g | *Macromolecules* 2014, 47, 2037−2043

cylindrical arrangement. A critical factor controlling the morphology is the volume fraction of PS (f_{PS}).

It is well-known that linear AB or ABA block copolymers show a nearly symmetric phase diagram.[3] A lamellar morphology appears in a large composition range centered around f_A = 0.5. Double gyroid, hexagonally packed cylinder (HEX), and body-centered cubic sphere (BCC) morphologies consisting of A domains in the B matrix usually emerge in that sequence as f_A is decreased from 0.5. The corresponding morphologies appear on the other side of the phase diagram with reversed phases. For SI and SIS linear block copolymers,[4] the phase boundaries in the strong segregation limit are PS BCC spheres, $f_{PS} < 0.17$; PS HEX, $0.17 < f_{PS} < 0.28$; PS double gyroid, $0.28 < f_{PS} < 0.34$; lamellae, $0.34 < f_{PS} < 0.62$; PI double gyroid, $0.62 < f_{PS} < 0.66$; PI HEX, $0.66 < f_{PS} < 0.77$; PI BCC, $f_{PS} > 0.77$. Commercial SIS-based TPEs have therefore a maximum PS fraction of 0.3 in order to remain elastic.

Since overall molecular weight is often limited by synthetic or processing constraints, f_{PS} is also a key factor that relates to the elastic recovery and ultimate strain at break of the TPE. To be an elastomer, the PS blocks should assemble as a discrete phase in a rubbery matrix with either spherical or cylindrical morphology. As a result, the present commercial TPEs have a low limiting value of $f_{PS} < 0.3$ for recoverable elasticity. Accordingly, the PS blocks in commercial SIS are relatively short, producing a decreased glass transition temperature (T_g) of the PS domains, thus allowing pull-out of the PS end blocks from these domains.[5,6] A conventional approach to enhance the mechanical stability of the PS domain is to blend SIS with another homopolymer that segregates specifically in the PS domains and has an even higher glass transition temperature [such as poly(phenylene oxide), PPO].[7,8] Yet, this method does not lift the volume fraction limitation, and the total hard phase fraction $f_{PS} + f_{PPO}$ must still remain below approximately 0.3.

Being able to significantly displace the classical phase diagram and stabilize morphologies with discrete PS domains while increasing f_{PS} above 0.3 would therefore constitute a technological breakthrough. Over the past two decades, it has been realized that asymmetric block copolymer architectures can significantly shift phase boundaries.[3,9−13] This suggests that block copolymers with appropriate asymmetric architectures could contain exceptionally high hard block fraction, and still yield elastomers, thus providing a unique combination of high modulus, toughness, and recoverable elasticity. On the basis of this idea and using previous self-consistent field theory (SCFT) simulations as a guide,[14] we designed a series of linear triblock [SIS′, S and S′ indicate long and short polystyrene blocks, respectively, and I denotes polyisoprene (PI)] and miktoarm [$S(IS')_2$ and $S(IS')_3$] block copolymers with asymmetric architectures. Crucially, we fixed the ratio of the S block length to the sum of the S and S′ block lengths, $\tau = N_S/(N_S + N_{S'}) = 8/9 \approx 0.89$, which was identified in the SCFT studies as yielding maximum deflection of the (PS cylinder) HEX phase to higher total PS volume fraction f_{PS}. In this study, we confirm experimentally that HEX morphologies with PS cylinders can indeed be achieved at f_{PS} significantly greater than 0.3, while preserving high extension and good elastic recovery. Also, due to the specific molecular architecture, the $S(IS')_3$ miktoarm block copolymers assembled with a much smaller domain spacing than the corresponding linear block copolymers.

EXPERIMENTAL SECTION

The three block copolymer architectures are schematically illustrated in Figure 1. All samples have the same long PS block (about 80 kg/mol) and different numbers of PI-*b*-PS diblock arms with short PS terminal blocks (approximately 10 kg/mol). The long and short PS blocks are connected by PI midblocks to give linear and star architectures. The total volume fractions of PS are kept constant across the three architectures, and three values were targeted in the samples reported here: f_{PS} = 0.4, 0.5, and 0.7, respectively. The synthesis method and detailed characterization can be found in the Supporting Information (Part A) and in the literature.[15]

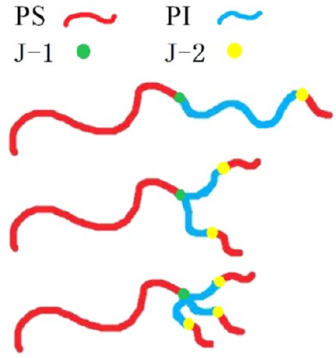

Figure 1. Molecular architectures of the linear and miktoarm block polymers. J-1 and J-2 indicate two kinds of junction points.

The morphologies of all neat block copolymers were characterized by transmission electron microscopy (TEM) and small-angle synchrotron X-ray scattering (SAXS). The samples were first annealed at 150 °C for 48 h in a high-vacuum chamber (10^{-8} mbar) to achieve thermal equilibrium. Ultrathin (~100 nm) sections were cut by a cryo-ultramicrotome at −90 °C and then stained in osmium tetroxide vapors to enhance the contrast for TEM. The SAXS experiments were carried out using the Advanced Light Source beamline 7.3.3 at Lawrence Berkeley National Laboratory. The X-ray wavelength of the beam is 0.124 nm.

Monotonic and step-cycle tensile mechanical tests were carried out with 7−10 dog-bone-shaped specimens to provide a good statistical representation. The gauge length of each specimen was 7 mm long and has a cross section that is 2 mm wide and 0.6−0.8 mm thick. The crosshead speed of the tensile machine was kept at 5 mm/min for all the testing, which produced a strain rate of 0.012 s^{-1}.

RESULTS AND DISCUSSION

Morphologies. The microphase-separated structures are shown in Figure 2 for linear SIS′ and miktoarm $S(IS')_3$ block copolymers with different compositions. The linear block copolymers show lamellar structures when f_{PS} is 0.4 or 0.5, which is consistent with reported morphologies for SI or (symmetric) SIS block copolymers.[4] When f_{PS} is increased to 0.7, an inverse HEX phase with PI cylinders is expected for conventional symmetric SIS triblock copolymers, but the gyroid structure was obtained in our SIS′ block copolymer, which indicates the phase diagram is shifted slightly by the asymmetry of the SIS′. Indeed, this shift has been predicted by Matsen by SCFT simulations for ABA′ triblocks,[13] although χN for the present samples greatly exceeds the segregation strengths explored in the simulations. (The values of χN for the linear BCPs with f_{PS} of 0.4, 0.5, and 0.7 are 211, 179, and 119, respectively. At 150 °C χ = 0.049 based on a reference volume of 0.1 nm^3.[16])

In contrast, the miktoarm block copolymers formed significantly different structures from the linear SIS′ at each

dx.doi.org/10.1021/ma402566g | *Macromolecules* 2014, 47, 2037−2043

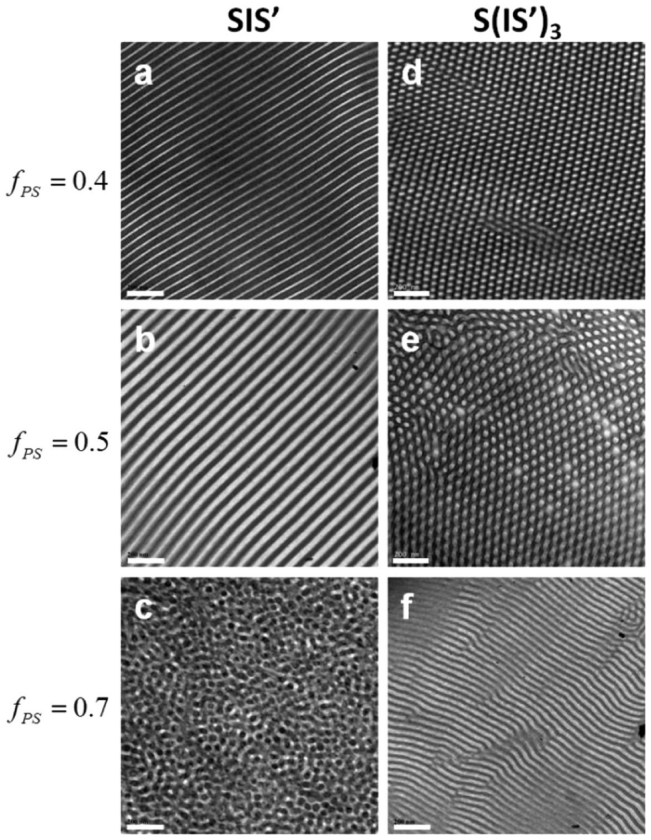

Figure 2. Characteristic microphase-separated structures revealed by TEM in linear and miktoarm block copolymers with different volume fractions of PS (white). The scale bars correspond to 200 nm.

corresponding composition. A HEX phase with PS cylinders embedded in the PI matrix is seen for the $S(IS')_3$ when f_{PS} = 0.4 or 0.5. The $S(IS')_3$ with f_{PS} = 0.7 is a lamellar structure, consisting of thick PS and thin PI layers. These results show that the phase diagram is dramatically shifted in asymmetric miktoarm block copolymers to produce ordered phases with a continuous elastomeric matrix and discrete PS domains at high f_{PS}. Moreover, the observed morphologies are in excellent agreement with our previously published SCFT phase diagram for the $A(BA')_3$ architecture,[14] although again the segregation strength of the present samples is considerably higher than the value used in the simulations. (The values of χN for miktoarm BCPs with f_{PS} at 0.4, 0.5, and 0.7 are 132, 108, and 95, respectively. N is defined as the number of statistical segments in an S−I−S′ linear strand with reference volume 0.1 nm^3.[16]) As expected, the $S(IS')_2$ architecture produces phases that are shifted an intermediate amount in f_{PS} (see Figure S2 in Supporting Information).

SAXS provides an overall statistical characterization of the bulk block copolymer morphology that is complementary to the local structures provided by the TEM micrographs. As shown in Figure 3, the lamellar, gyroid, and cylinder structures are revealed by the q/q^* ratios (q^* is the primary peak position).[17] These high-resolution SAXS results confirm that the rightmost phase boundary for the cylindrical structure has been shifted to much higher PS fractions in miktoarm $S(IS')_3$ block copolymers, which is consistent with the TEM observations and our previous simulation work.[14] In contrast, the microphase-separated structures are less shifted in SIS′ and

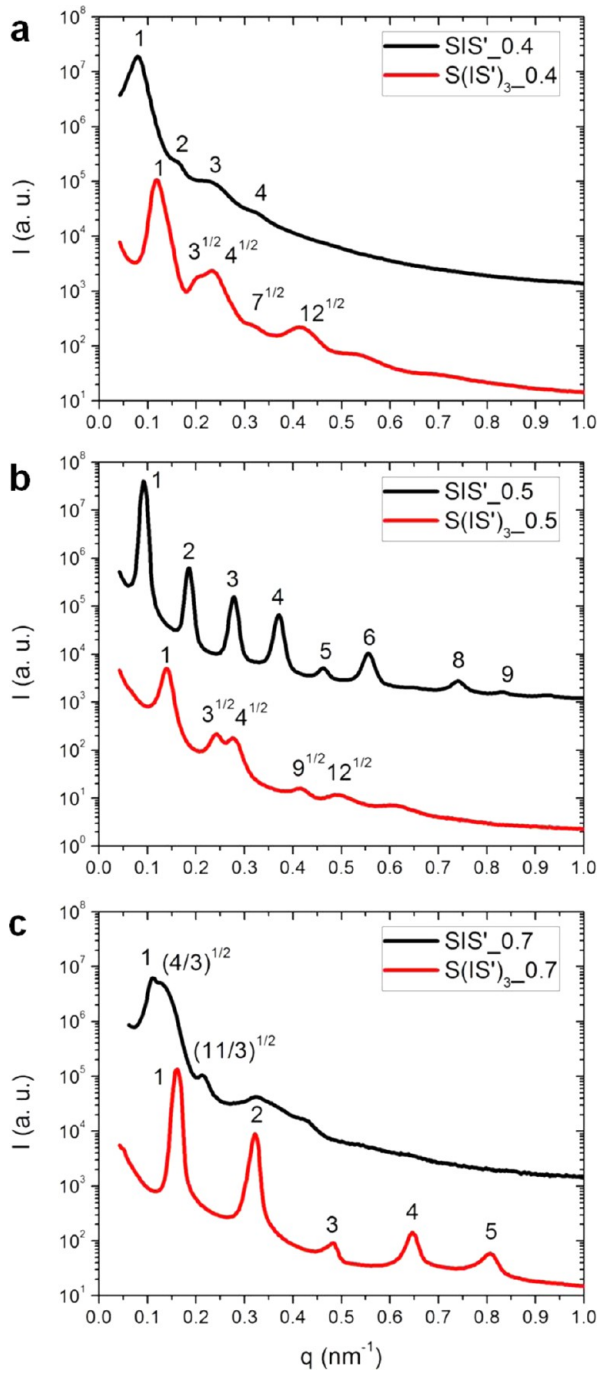

Figure 3. Small-angle synchrotron X-ray scattering curves for linear and miktoarm block copolymers with different volume fractions of PS (a, b, and c correspond to f_{PS} = 0.4, 0.5, and 0.7, respectively).

$S(IS')_2$ block copolymers (see Figure S2 in Supporting Information for the $S(IS')_2$ SAXS data).

The domain plane spacings ($L = 2\pi/q^*$) can also be identified from Figure 3. The L values for linear BCPs with f_{PS} = 0.4, 0.5, and 0.7 are 80.6 ± 2.2, 68.7 ± 1.7, and 56.2 ± 1.1 nm, respectively. The corresponding values for the miktoarm BCPs are 53.0 ± 1.0, 45.2 ± 0.7, and 38.9 ± 0.5 nm. Since the molecular weights of the long and short PS blocks are kept the same in all samples, the total molecular weight of each miktoarm BCP is larger than the corresponding linear one. But the miktoarms give much smaller domain spacings. We will discuss this later.

dx.doi.org/10.1021/ma402566g | Macromolecules 2014, 47, 2037−2043

It has been predicted and shown experimentally that the asymmetry in molecular architecture may induce the shift of phase boundaries.[3,9−13] The $A(BA')_n$ architecture is unusual in that two different physical mechanisms combine to drive strong curvature toward A domains and hence enhance the stability of discrete domain structures to high f_A.

In symmetric ABA or A_mB_n ($m = n$) type of block copolymers,[3,17] a junction point connects equal numbers of A and B blocks. When the junction point is located at the interface between A-rich and B-rich phases, the spontaneous interfacial curvature is sensitive to the volume ratio of the two kinds of blocks. The short blocks stay in a concave geometry, and the long blocks populate the matrix on the convex side to relieve their conformational entropy loss due to brush confinement. A flat interface is favored when the two block sizes are comparable.

In our asymmetric miktoarm block copolymers, there are two kinds of junction points. The first junction point (J-1) connects one long PS block and three PI blocks (for $n = 3$). The higher surface density of PI blocks near the interface would carry a large conformational entropy loss due to crowding if the interface were flat, so to lower its free energy the interface is driven to bend away from the PI domains, placing PI on the convex side of the interface. This is the same mechanism responsible for shifting phase boundaries in A_mB_n ($m < n$) block copolymers with single junction points,[3,9−13] although it should be noted that polymers in this class, e.g. SI_2 or SI_3, have no mechanical strength or potential for use as TPEs because the elastomeric soft blocks are not anchored at both ends. In contrast, the $S(IS')_3$ architecture has both ends of the soft PI blocks anchored in glassy PS, the terminal end anchoring provided by a second junction point (J-2) that connects on each diblock arm one short PS block to one PI block terminus. In the strong segregation limit ($\chi N > 40$, where N is the number of statistical segments in an S−I−S′ linear strand), J-2 is also located at the interface.[14,19] The short PS blocks populate the interfacial region of the PS domains but contribute less conformational entropy penalty per unit volume than the long PS blocks. This dilutes the density of long PS blocks near the interface and thus assists the conformation relaxation. So J-2 plays an additional role in stabilizing the PS phase with a concave curvature, which can be considered as a "polydisperse PS brush"[20,21] or a "surfactant" effect.[22,23] Notably, the $S(IS')_3$ architecture produces not only stronger deflections of the phase boundaries to higher f_{PS} than a corresponding SI_3 polymer but also offers the potential for a practical TPE material.

The role of J-1 is diminished in $S(IS')_2$ and lost entirely in SIS′ linear block copolymers. The polydisperse brush effect associated with J-2 is also decreased upon reducing n because of a lower ratio of short to long PS blocks. As a consequence, the phase boundary shifts are not as pronounced in $S(IS')_2$ and SIS′. A useful architectural parameter that (along with n, χN, and f_{PS}) dictates the phase diagram asymmetry is the block length ratio $\tau = N_S/(N_S + N_{S'})$, the ratio of the long PS block length to the sum of the long and short PS block lengths. When τ approaches 0, the role of J-1 is lost, and we have an $(IS)_n$ radial star block copolymer. In contrast, the role of J-2 is lost when τ approaches 1, the limit corresponding to a SI_n miktoarm star copolymer. As the J-1 and J-2 conformational entropy effects are reinforcing, we would anticipate the largest phase boundary deflections for intermediate τ. The optimal value of τ was identified to be about 0.9 in our previous SCFT simulation work (Figure 7 in ref 14). It is crucial, however, to emphasize that a $S(IS')_3$ miktoarm block copolymer with $\tau = 0.9$ should be far superior mechanically to a ($\tau = 1$) SI_3 miktoarm star copolymer due to the multiple anchoring S′ blocks.

Here we further point out that the roles of J-1 and J-2 are responsible for the small domain spacings and sizes of the miktoarm BCPs. We limit our discussion in the strong segregation regime where the junction points are located in sharp interfaces. Here the comparison is made among a set of five molecular architectures (Figure 4): AB, ABA′, ABA, AB_3, and $A(BA')_3$, with assumption of the same total molecular weight and same composition $f_A = 0.5$. Because of the crowding of segments and the enthalpic repulsion, each block is most stretched near the junction point and adopts more conformational freedom farther away. The AB diblock copolymer has the constraint only from one junction point. Each block free end has the most optimum distribution near the center of the corresponding block domain. The thickness of each block domain can be considered to be approximately twice the corresponding extended block size. The domain size usually follows the simple power relation $L_{AB} \sim (N_A + N_B)^{2/3}$. When there is a second junction point J-2 within the chain, as in the ABA′ block copolymer, the middle B blocks are anchored as bridges or loops. In this case, the thickness of the B domain can be considered to be the size of one stretched B block (more stretched than the B block in an AB diblock). The thickness of the A-rich domain is mainly determined by the longer block of A or A′. When A equals A′, the symmetric ABA triblock copolymer has a domain size slightly larger than $^1/_2L_{AB}$.[13] Compared with an AB diblock copolymer, the AB_3 miktoarm BCP (at the same f_A) has approximately the same domain size of the A-rich domain but decreased size of the B-rich domain. Naively, we would expect a relation $L_{AB_3} \sim (N_A + N_B/3)^{2/3}$. But due to the large segment density near J-1, each short B branch is significantly stretched. Accordingly, the actual domain size is much larger.[9]

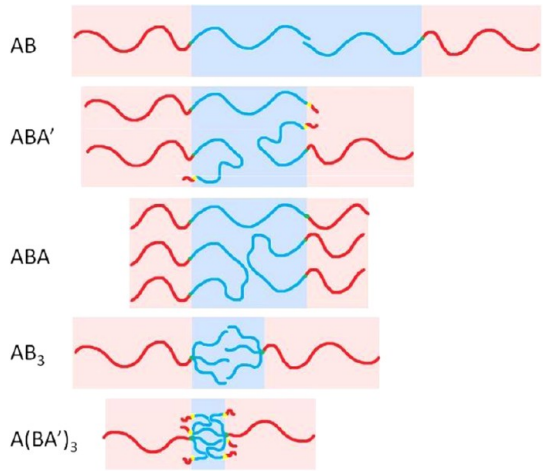

Figure 4. Schematic illustration of the domain sizes with different molecular architectures. The red region indicates the A-rich phase and the blue is the B-rich phase.

Compared with the AB_3 miktoarm, the three additional J-2 junctions in $A(BA')_3$ anchor the B blocks with bridges or loops, further reducing the B-rich domain size. Here, we further point out that the location of the short A′ blocks near the interface also relieve the crowding within the domain so that the long A blocks are not as stretched as those in an AB_3 miktoarm or

dx.doi.org/10.1021/ma402566g | Macromolecules 2014, 47, 2037−2043

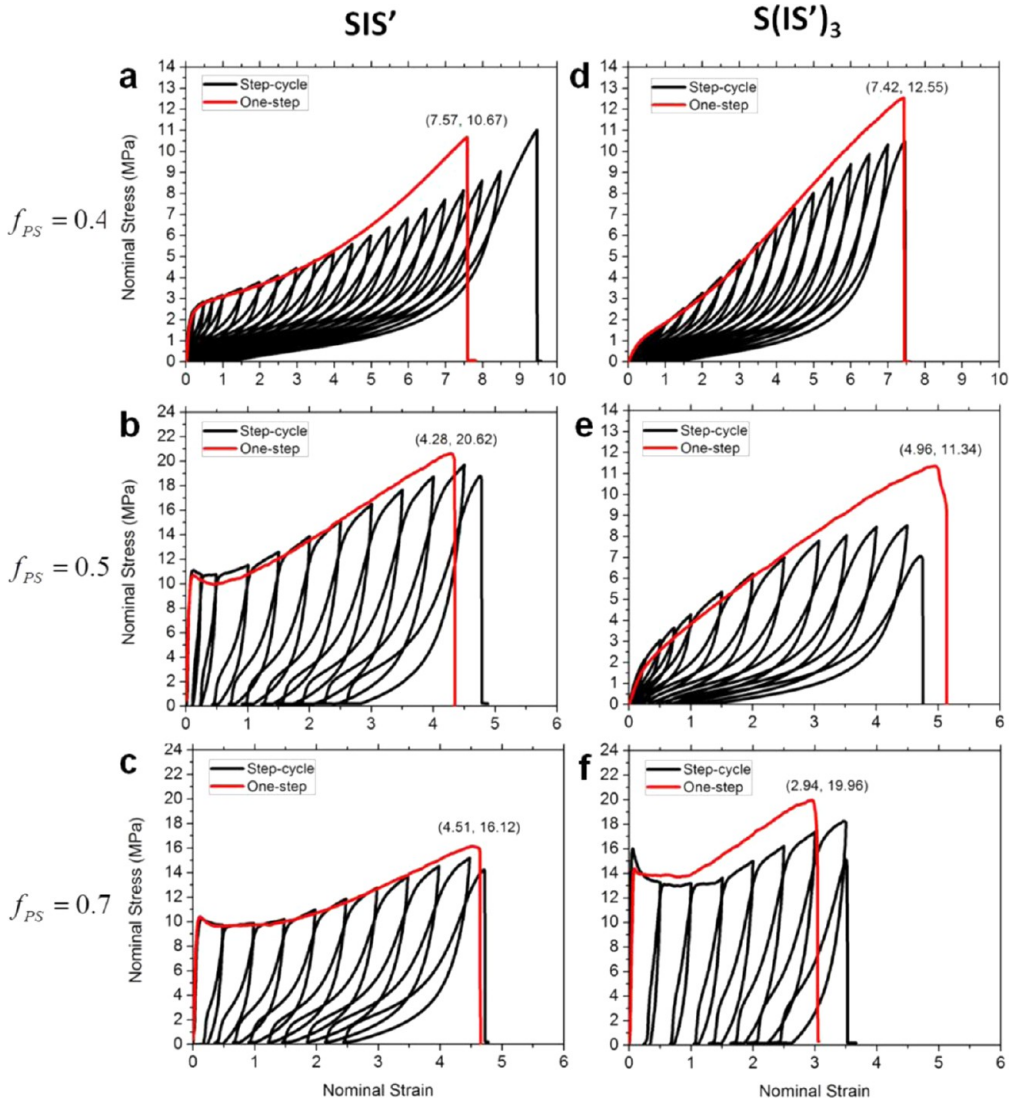

Figure 5. Monotonic and cyclic tensile testing data for linear and miktoarm block copolymers with different volume fractions of PS.

ABA′ linear block copolymer. The thickness of the PS domains in lamellar structures can be estimated with the long period from SAXS and the volume fraction (Table S1). In linear SIS′ with f_{PS} = 0.4 (N_{PS} = 1559 and d = 80.6 nm), the thickness of the PS domains is about 30.6 nm. In linear SIS′ with f_{PS} = 0.5 (N_{PS} = 1738 and d = 68.7 nm), the PS domain thickness is about 35.0 nm. The latter is larger because of the larger PS molecular weight (Table S1). In contrast, in miktoarm $S(IS')_3$ with f_{PS} = 0.7 (N_{PS} = 1970 and d = 38.9 nm), the thickness of PS lamellar domain is about 26.1 nm, much smaller than the values of the linear polymers even though the molecular weight is larger. In summary, $A(BA')_3$ miktoarms have significantly smaller domain sizes at comparable f_A and molecular weight due to the concerted influence of the two types of junction points (J-1 and J-2). As there are more anchoring points in $A(BA')_3$ miktoarms, we would expect better mechanical properties than the corresponding AB, ABA′, and AB_3 copolymers. This is a subject to which we now turn.

Mechanical Properties. The asymmetric miktoarm block copolymers have interesting mechanical properties that reflect their architecture and morphologies. The tensile testing data are shown in Figure 5.

The linear SIS′ block copolymers generally behave like rigid plastics when f_{PS} > 0.4. For the samples with f_{PS} = 0.5 or 0.7, there is clear indication of yielding in the tensile curves at about 10 MPa. During the tensile experiment, neck formation occurs at the small strains beyond yield. The Young's moduli for these two samples are about 200 MPa. The plastic deformation is more clearly revealed by the step-cycle tensile testing curves, which show that a large part of total strain does not recover after the load is removed. From Figure 2, we know this mechanical behavior results from the deformation of continuous lamellar or gyroid PS domains.[24] The mechanical behavior is more complex for the linear polymer with f_{PS} = 0.4. Although the minor PS domain forms a lamellar structure, the thin PS lamellae can be easily broken into dispersed fragments at large strains. This process is usually called a "plastic-to-rubber" transition and can lead to higher recovery of the total strain (Figure S3 in Supporting Information).[25]

The miktoarm $S(IS')_3$ block copolymer with f_{PS} = 0.7 shows yielding and extensive plastic deformation as expected from its lamellar morphology. The thick PS lamellae increase the yield stress to approximately 15 MPa. When the PS content is lowered to 0.5, PS domains form cylinders in the continuous PI rubbery matrix. As a result, this sample shows overall excellent

dx.doi.org/10.1021/ma402566g | Macromolecules 2014, 47, 2037−2043

mechanical behavior with initial Young's moduli equal to 12.3 ± 0.3 MPa, high stresses and strains at break, and good elastic recovery as shown in Figures 5 and 6. While the elastic recovery

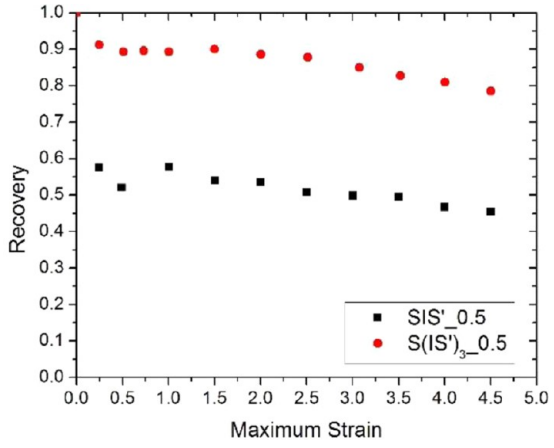

Figure 6. Elastic recovery of linear SIS′ and miktoarm block copolymers $S(IS')_3$ with f_{PS} = 0.5.

for the $S(IS')_3$ miktoarm block copolymer with f_{PS} = 0.5 is over 80% after a strain of 4, the elastic recovery of the linear SIS′ with the same f_{PS} is less than 50% after the same maximum strain. The elastic recovery of the miktoarm block copolymer is approximately 90% when the maximum strain is smaller than 2.5. Similarly, the miktoarm block copolymer $S(IS')_3$ with f_{PS} = 0.4, which also has the HEX morphology with PS cylinders, has Young's moduli of 3.5 ± 0.3 MPa, an ultimate strain to break over 7 and an elastic recovery of better than 90% before a maximum strain of 6 (Figure S3 in Supporting Information).

Evidently, the most striking advantage of the miktoarms is the significantly enhanced strength and recoverable elasticity at high content of PS in comparison to linear SIS and SIS′ copolymers. In conventional SIS linear triblock copolymer elastomers with symmetric end blocks, due to the low fraction of the glassy phase, the stress at 300% strain is usually relatively small (~1 MPa for f_{PS} = 0.16 and ~2.5 MPa for f_{PS} = 0.28).[5,26] The corresponding values are 4.6 ± 0.1 and 8.1 ± 0.2 MPa in miktoarms with f_{PS} = 0.4 and 0.5, respectively. The strength, toughness, and elasticity are evidently well-balanced in these materials.

The mechanical behavior of miktoarm block copolymers is intrinsically determined by the molecular architecture. The $S(IS')_3$ architecture with J-1 and J-2 junctions and appropriate block ratio τ enables a high volume fraction of glassy PS to be stabilized as a discrete HEX phase in a continuous PI rubbery matrix. This nanostructure is a necessary condition for elastic behavior, but sufficiency is provided by the anchoring S and S′ blocks that contribute strength and recoverable elasticity.

We should mention two potential drawbacks in the molecular design. Compared with a single long PI block in the linear architecture, there are three short PI blocks in a $S(IS')_3$ miktoarm block copolymer. This results in PI domains that are less deformable under stress. On the other hand, the J-2 junctions between the PI blocks and the short PS tails supply more anchoring points. The short PS blocks can be easily pulled out of the glassy domains at large strains and might play a role as a sacrificial component. This accommodates the overloaded stress on local scales, but it is a time-dependent plastic contribution that evidently contributes to "strain softening" in step-cycle tensile testing and decreasing recovery at large strains. It will be of interest to study the mechanical properties of related $S(IS')_n$ systems with larger n (>3), where SCFT studies suggest even more extreme deflections of the HEX−gyroid phase boundary.[14] The further shortening of the PI blocks and increased degeneracy of anchoring will undoubtedly influence the nonlinear mechanical properties in interesting and potentially surprising ways.

■ CONCLUSIONS

In summary, we have shown that hexagonal cylinders with PS as the discrete domain can be achieved with unusually high PS volume fractions, up to 0.5, by using $S(IS')_3$ miktoarm block copolymer architectures with an approximately 8:1 ratio of PS to PS′ block lengths. These polymers exhibit strong, tough, and elastic mechanical properties. This work shows that block copolymers with asymmetric architectures have considerable potential in improving the mechanical performances of standard TPEs as well as in creating new families of tougher, stronger, and elastic materials.

A straightforward and very promising future direction consists in blending the miktoarm block copolymers with a second polymer component, such as PS homopolymer.[27−29] Compared with the traditional SIS triblock copolymer, it should be possible to accommodate a much larger amount of a PS-compatible, rigid polymer additives into the PS domains, while maintaining them discrete. Such blends could further enhance the modulus and strength while preserving toughness and recoverable elasticity.

■ ASSOCIATED CONTENT

Supporting Information

Part A: chemical synthesis and molecular characterization; Part B: structures in $S(IS')_2$; Part C: recovery of SIS′ and $S(IS')_3$ with f_{PS} = 0.4. This material is available free of charge via the Internet at http://pubs.acs.org.

■ AUTHOR INFORMATION

Corresponding Authors

*E-mail edkramer@mrl.ucsb.edu (E.J.K.).
*E-mail ghf@mrl.ucsb.edu (G.H.F.).
*E-mail aavger@cc.uoi.gr (A.A.).

Notes

The authors declare no competing financial interest.

■ ACKNOWLEDGMENTS

This research was supported by the Institute for Collaborative Biotechnologies through grant W911NF-09-0001 from the U.S. Army Research Office. The content of the information does not necessarily reflect the position or the policy of the Government, and no official endorsement should be inferred. Extensive use was made of the MRL Shared Experimental Facilities supported by the MRSEC Program of the NSF under Award DMR 1121053; a member of the NSF-funded Materials Research Facilities Network.

■ REFERENCES

(1) Bates, F. S.; Fredrickson, G. H. *Phys. Today* **1999**, *52*, 32.
(2) Bates, F. S.; Fredrickson, G. H. *Annu. Rev. Phys. Chem.* **1990**, *41*, 525.
(3) Matsen, M. W. *Macromolecules* **2012**, *45*, 2161.
(4) (a) Khandpur, A. K.; Förster, S.; Bates, F. S.; Hamley, I. W.; Ryan, A. J.; Bras, W.; Almdal, K.; Mortensen, K. *Macromolecules* **1995**,

28, 8796. (b) Avgeropoulos, A.; Dair, B. J.; Hadjichristidis, N.; Thomas, E. L. *Macromolecules* **1997**, *30*, 5634.
(5) Zhao, Y.; Ning, N.; Hu, X.; Li, Y.; Chen, F.; Fu, Q. *Polymer* **2012**, *53*, 4310.
(6) Weidisch, R.; Gido, S. P.; Uhrig, D.; Iatrou, H.; Mays, J.; Hadjichristidis, N. *Macromolecules* **2001**, *34*, 6333.
(7) Puskas, J. E.; Kwon, Y.; Altstädt, V.; Kontopoulou, M. *Polymer* **2007**, *48*, 590.
(8) Tucker, P. S.; Barlow, J. W.; Paul, D. R. *Macromolecules* **1988**, *21*, 1678.
(9) Dyer, C.; Driva, P.; Sides, S. W.; Sumpter, B. G.; Mays, J. W.; Chen, J.; Kumar, R.; Goswami, M.; Dadmun, M. D. *Macromolecules* **2013**, *46*, 2023.
(10) Grason, G. M.; Kamien, R. D. *Macromolecules* **2004**, *37*, 7371.
(11) Beyer, F. L.; Gido, S. P.; Velis, G.; Hadjichristidis, N.; Tan, N. B. *Macromolecules* **1999**, *32*, 6604.
(12) Milner, S. T. *Macromolecules* **1994**, *27*, 2333.
(13) Matsen, M. W. *J. Chem. Phys.* **2000**, *113*, 5539.
(14) Lynd, N. A.; Oyerokun, F. T.; O'Donoghue, D. L.; Handlin, D. L., Jr.; Fredrickson, G. H. *Macromolecules* **2010**, *43*, 3479.
(15) Avgeropoulos, A.; Hadjichristidis, N. *J. Polym. Sci., Part A: Polym. Chem.* **1997**, *35*, 813.
(16) Balsara, N. P.; Eitouni, H. B. Thermodynamics of Polymer Blends. In *Physical Properties of Polymers Handbook*, 2nd ed.; Mark, J. E., Ed.; Springer: New York, 2007; Chapter 19, pp 339−356.
(17) Hamley, I. W.; Castelletto, V. *Prog. Polym. Sci.* **2004**, *29*, 909.
(18) Zhu, Y.; Gido, S. P.; Moshakou, M.; Iatrou, H.; Hadjichristidis, N.; Park, S.; Chang, T. *Macromolecules* **2003**, *36*, 5719.
(19) Mayes, A. M.; Johnson, R. D.; Russell, T. P.; Smith, S. D.; Satija, S. K.; Majkrzak, C. F. *Macromolecules* **1993**, *26*, 1047.
(20) Milner, S. T.; Witten, T. A.; Cates, M. E. *Macromolecules* **1989**, *22*, 853.
(21) Dan, N.; Tirrell, M. *Macromolecules* **1993**, *26*, 6467.
(22) Court, F.; Yamaguchi, D.; Hashimoto, T. *Macromolecules* **2008**, *41*, 4828.
(23) Court, F.; Hashimoto, T. *Macromolecules* **2001**, *34*, 2536.
(24) Cohen, Y.; Albalak, R. J.; Dair, B. J.; Capel, M. S.; Thomas, E. L. *Macromolecules* **2000**, *33*, 6502.
(25) Adhikari, R.; Michler, G. H. *Prog. Polym. Sci.* **2004**, *29*, 949.
(26) Schlegel, R.; Wilkin, D.; Duan, Y.; Weidisch, R.; Heinrich, G.; Uhrig, D.; Mays, J. W.; Iatrou, H.; Hadjichristidis, N. *Polymer* **2009**, *50*, 6297.
(27) Mezzenga, R.; Ruokolainen, J.; Fredrickson, G. H.; Kramer, E. J.; Moses, D.; Heeger, A. J.; Ikkala, O. *Science* **2003**, *299*, 1872.
(28) Patel, R. M.; Hahn, S. F.; Esneault, C.; Bensason, S. *Adv. Mater.* **2000**, *12*, 1813.
(29) Avgeropoulos, A.; Dair, B. J.; Thomas, E. L.; Hadjichristidis, N. *Polymer* **2002**, *43*, 3257.